

Molecular phenotypes reveal heterogeneous engraftments of patient-derived hepatocellular carcinoma xenografts

Jianyong Zhuo^{1,2,3*}, Di Lu^{1*}, Jianguo Wang¹, Zhengxing Lian³, Jiali Zhang³, Huihui Li³, Beini Cen³, Xuyong Wei¹, Qiang Wei¹, Haiyang Xie³, Xiao Xu^{1,2,3}

¹Department of Hepatobiliary and Pancreatic Surgery, The Center for Integrated Oncology and Precision Medicine, Affiliated Hangzhou First People's Hospital, Zhejiang University School of Medicine, Hangzhou 310003, China; ²Department of Hepatobiliary and Pancreatic Surgery, the First Affiliated Hospital, Zhejiang University School of Medicine, Hangzhou 310003, China; ³National Health Commission Key Laboratory of Combined Multi-organ Transplantation; Institute of Organ Transplantation, Zhejiang University, Hangzhou 310003, China

*These authors contributed equally to this work.

Correspondence to: Xiao Xu. Department of Hepatobiliary and Pancreatic Surgery, The Center for Integrated Oncology and Precision Medicine, Affiliated Hangzhou First People's Hospital, Zhejiang University School of Medicine; Department of Hepatobiliary and Pancreatic Surgery, the First Affiliated Hospital, Zhejiang University School of Medicine; National Health Commission Key Laboratory of Combined Multi-organ Transplantation; Institute of Organ Transplantation, Zhejiang University, Hangzhou 310003, China. Email: zjxu@zju.edu.cn.

Abstract

Objective: Patient-derived xenograft (PDX) models provide a promising preclinical platform for hepatocellular carcinoma (HCC). However, the molecular features associated with successful engraftment of PDX models have not been revealed.

Methods: HCC tumor samples from 76 patients were implanted in immunodeficient mice. The molecular expression was evaluated by immunohistochemistry. Patient and tumor characteristics as well as tumor molecular expressions were compared for PDX engraftment using the Chi-square test. The independent prediction parameters were identified by logistic regression analyses.

Results: The engraftment rate for PDX models from patients with HCC was 39.47% (30/76). Tumors from younger patients and patients with elevated preoperative alpha-fetoprotein level had higher engraftment rates. Tumors with poor differentiation and vascular invasion were related to engraftment success. The positive expression of CK19, CD133, glypican-3 (GPC3), and Ki67 in tumor samples was associated with engraftment success. Logistic regression analyses indicated that GPC3 and Ki67 were two of the strongest predictors of PDX engraftment. Tumors with GPC3/Ki67 phenotypes showed heterogeneous engraftment rates, with 71.9% in GPC3⁺/Ki67⁺ tumors, 30.8% in GPC3⁻/Ki67⁺ tumors, 15.0% in GPC3⁺/Ki67⁻ tumors, and 0 in GPC3⁻/Ki67⁻ tumors.

Conclusions: Successful engraftment of HCC PDXs was significantly related to molecular features. Tumors with the GPC3⁺/Ki67⁺ phenotype were the most likely to successfully establish HCC PDXs.

Keywords: Hepatocellular carcinoma; patient-derived xenografts; heterogeneous establishment; molecular phenotype

Submitted Apr 08, 2021. Accepted for publication Jul 20, 2021.

doi: 10.21147/j.issn.1000-9604.2021.04.04

View this article at: <https://doi.org/10.21147/j.issn.1000-9604.2021.04.04>

Introduction

Hepatocellular carcinoma (HCC) is the third most fatal

cancer worldwide and causes over 740,000 deaths annually (1,2). More than 50% of the new HCC cases and deaths occur in China, which causes a huge burden to China (3,4).

Only a small number of patients with HCC are suitable for surgery with 60%–70% of patients losing their chance of surgical intervention at the time of diagnosis (2,5). Systemic therapy, including four multi-target tyrosine kinase inhibitors, is the first treatment option for patients with advanced HCC. However, the response to molecule-targeted drugs varies among patients (1,6,7). This heterogeneous treatment response highlights the need for developing effective personalized therapy for patients with HCC through precision medicine. To overcome the limitation, more realistic models are needed to study the therapeutic response of specific molecular-subtypes of HCC. Despite their merits, traditional cancer cell lines and cell-derived xenograft models have failed to assist clinical decisions because they are adapted to plastic culture conditions, therefore, have lost the ability to represent the genetic, transcriptional, and epigenetic heterogeneity of patient tumors (8).

Patient-derived xenograft (PDX) models are regarded as more realistic cancer models for exploring therapeutic strategies. PDX tumors recapitulate the histopathology, genomic expression, and treatment response of the corresponding patients' primary tumors (9). Recently, PDX models have gained attention and are commonly being used for the development of effective treatments against various cancers in both academic and pharmaceutical institutions (9,10). However, the unstable engraftments of PDXs limit its applicability, regardless of the prospect of PDX models for mechanism research and aiding clinical translation. Some cancer types, such as colorectal and breast cancer and pancreatic ductal adenocarcinoma, demonstrate high engraftment rates (11,12). However, the engraftment rate of HCC PDXs is approximately 40%, which is lower than that of other cancer types (13,14). Additionally, parameters

correlated with successful engraftment of HCC PDXs are not clear. Therefore, we aimed to identify the important pathological and molecular factors related to the engraftment of HCC PDX models.

Materials and methods

Patients and tumor samples

The study was approved by the Medical Ethics Committee of the First Affiliated Hospital, Zhejiang University School of Medicine. All patients provided written informed consent before surgery. HCC tissue samples were obtained between March 2017 and March 2019. Fresh tumor specimens were transferred in ice-chilled Dulbecco's Modified

Eagle Medium/Ham's F12 (DMEM/F12, Sigma, USA) supplemented with 100 U/mL penicillin and 100 U/mL streptomycin for engraftment. The remaining tumor specimens were snap-frozen in liquid nitrogen and fixed in paraffin for future studies. A similar process was performed on tumors collected from mice. The overall procedure flow chart is shown in *Figure 1*.

Animals

Four- to five-week-old, male non-obese diabetic/severe combined immunodeficient (NOD/SCID) and NOD/SCID/IL-2 γ -receptor null (NSG) mice were purchased from Gempharmatech (Nanjing, China). All mice were maintained with 12-h light-dark cycles under specific pathogen-free conditions. All procedures were carried out in accordance with the Guide for the Care and Use of Laboratory Animals of the National Institutes of Health. Experiments were conducted with the approval of the

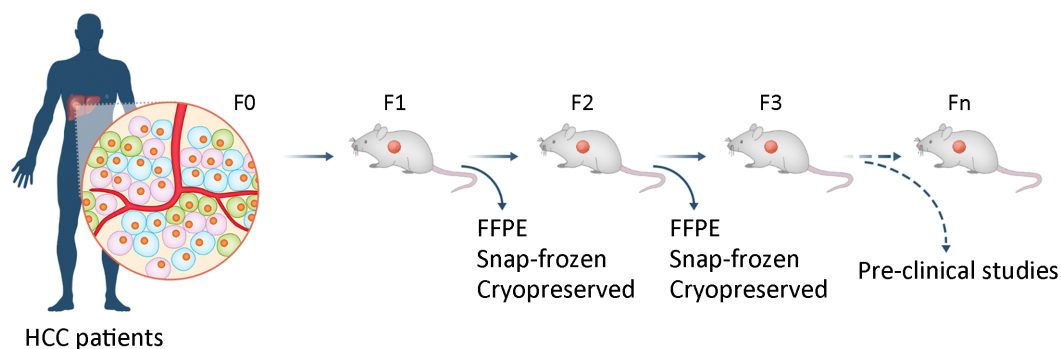


Figure 1 Schematic diagram of PDX program. PDX, patient-derived xenograft; HCC, hepatocellular carcinoma; FFPE, formalin-fixed and paraffin-embedded.

Ethics Committee of the First Affiliated Hospital, Zhejiang University School of Medicine and the Animal Care Committee of Zhejiang University School of Medicine.

Establishment of PDX models

The fresh tumor tissues were obtained from surgical room, and transferred into animal facility within 2 h. The primary tumor (F0) was divided into those to be implanted into immunodeficient mice, fixed in 10% formalin, and snap-frozen in liquid nitrogen. To establish PDX models, tumor pieces sized approximately 2 mm were subcutaneously implanted into the flanks of NOD/SCID or NSG mice with a trocar. Tumor growth was monitored twice weekly using a Vernier caliper and tumor volume (TV) was calculated as $TV = 0.5 \times \text{length} \times \text{width} \times \text{width}$. The established PDX model was termed F1, and subsequent generations were numbered consecutively (F2, F3, F4...). When the TV of F1 reached ~1,000 mm³, the mice were sacrificed. Tumor tissues were reinoculated to obtain subsequent generations, and remaining tissues were cryopreserved in liquid nitrogen for future resuscitation.

Hematoxylin and eosin (HE) staining and immunohistochemistry (IHC)

Tissue sample sections of 4- μ m thickness were prepared for HE staining and IHC. The diagnosis of HCC was confirmed by two pathologists, and IHC procedures for Ki67, alpha-fetoprotein (AFP), glypican-3 (GPC3), cytokeratin 19 (CK19), epithelial cell adhesion molecule (EpCAM) and cluster of differentiation 133 (CD133) were performed by the Department of Pathology, the First Affiliated Hospital, Zhejiang University School of Medicine.

Definition of histological patterns and positive expression of IHC makers

As previously described (15,16), the histological subtyping of tumors was divided into microtrabecular, macrotrabecular, pseudoglandular, compact pattern according to their architectural growth patterns. Expression of AFP, GPC3, EpCAM and CD133 with moderate or strong staining in tumor cells was defined as positive expression. Expression of CK19 with moderate or strong intensity in >5% of tumor cells was defined as CK19 positivity (17). The nuclear fraction of Ki67 positivity was quantitatively measured as previously described (18). The

cohort was divided into positive and negative Ki67 groups based on the cut-off value.

Statistical analysis

Statistical analyses were performed using IBM SPSS software (Version 23.0; IBM Corp., New York, USA). The relationship between successful establishment of PDXs and different parameters was analyzed using the Chi-square test. The predictive value of the parameters was determined using a receiver operating characteristic curve. The Mann-Whitney test was used to compare quantitative variables. Multivariate logistic regression was used to generate a model predicting the establishment of HCC PDXs. P-values <0.05 were considered significant.

Results

Baseline characteristics of primary tumors and related patients

We set up a complete flow for the construction of PDX models, and surgically fresh tumor tissues were implanted in immunodeficient mice. The established PDX model was termed F1, with subsequent generations numbered consecutively (F2, F3, F4...) (*Figure 1*). To obtain HCC PDXs, we implanted primary tumor tissues from 99 patients into immunodeficient mice. Twenty-three tumors were excluded because they were confirmed to be intrahepatic cholangiocarcinoma by postoperative pathology. Three other tumors were considered to be failed HCC PDXs because the F1 tumors were confirmed as lymphoma by pathologists. Finally, we enrolled 76 HCC PDXs for analysis, including 30 successful and 46 failed PDXs (*Figure 2*). In the cohort of HCC PDX models, the engraftment rate was 39.47% (30/76). The time to engraftment of six PDXs was not recorded, and the median time to engraftment of the remaining PDXs was 95 d with an interquartile range (IQR) of 62–123 d.

The baseline characteristics of the 76 patients are summarized in *Table 1*. The median age of all patients was 58.0 years, and 82.9% were male. Sixty-five (85.5%) patients had hepatitis B infection, and 48 (63.2%) patients had liver cirrhosis. Sixty-seven (88.2%) patients had primary tumors, and the remaining 9 (11.8%) patients had recurrent tumors. Twelve (15.8%) patients received trans-arterial chemoembolization before surgery, while the remaining 64 (84.2%) patients had not received any preoperative treatment. Forty-one (53.9%) patients

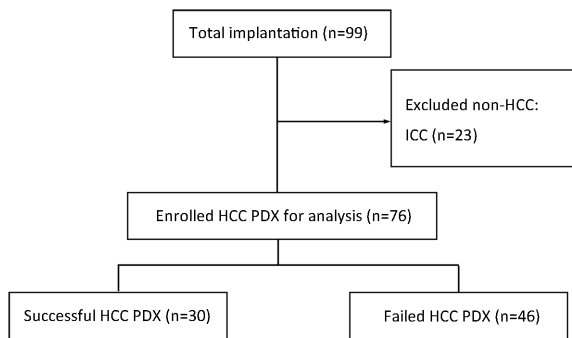


Figure 2 Design of analyzing parameters related to successful establishment of HCC PDXs. HCC, hepatocellular carcinoma; PDX, patient-derived xenograft; ICC, intrahepatic cholangiocarcinoma.

Table 1 Baseline characteristics of 76 patients and relatively primary tumor for HCC PDXs (N=76)

Characteristics	n/n
Age (year) (median, IQR)	58.0, 52.3–66.0
Sex (male/female)	63/13
Specimen (primary/recurrent)	67/9
Prior treatment (not received/received)	64/12
Preoperative AFP level (ng/mL) (median, IQR)	39.1, 5.9–382.2
Liver cirrhosis (yes/no)	48/28
Tumor size (≤5 cm/>5 cm)	51/25
Tumor differentiation (well/moderate/poor)	3/43/30
Satellite lesions (yes/no)	63/13
Vascular invasion (macro-/micro-/no)	11/20/45

HCC, hepatocellular carcinoma; PDX, patient derived xenograft; IQR, interquartile range; macro-, macrovascular; micro-, microvascular.

presented with elevated serum AFP (>20 ng/mL). There were 46 (60.5%) cases of well and moderate differentiation, and 30 (39.5%) cases of poor differentiation. Thirteen (17.1%) patients had satellite lesions. Forty-five (59.2%) patients had no vascular invasion, whereas twenty (26.3%) patients had microvascular invasion and eleven (14.5%) had macrovascular invasion.

PDXs preserve histopathology and molecular marker of primary tumors

HE staining revealed a similar cellular structure between F1 PDX tumors and primary tumors of the corresponding patients (Figure 3A). CK19 is regarded as a progenitor marker of HCC (19). CK19-positive HCC is a

characteristic subtype as it exhibits distinctive molecular profiling (20). Therefore, we assessed the consistency of CK19 expression between F0 and F1. In the successfully established PDX models, all F1 PDX tumors maintained CK19 expression of their matched primary tumors (Figure 3B). In PDX tumors, the expression of CK19 also remained unchanged after several passages (Figure 3C). These data implied that the xenografts recapitulated the histopathological features and expression of key molecules in the original tumors.

Mouse strains do not influence PDX establishment

Few studies have described parameters that influence the engraftment of HCC PDXs; therefore, we aimed to explore the relationship between the successful establishment and the parameters, including experimental parameters, clinicopathological parameters and molecular parameters. In the present study, tumors were directly implanted into the right flanks of immunodeficient mice without using Matrigel. Additionally, the exact overall procedure time of each PDX was not recorded. Therefore, we only compared relationship between the mouse strain and establishment rate. In the early phase, 53 PDXs were established in NOD/SCID mice. In the later phase, the remaining 23 PDXs were established in NSG mice. The data indicated that there was no difference between the two strains of mice (P=0.582, Table 2). Despite the lack of significance for engraftment, the median time to engraftment in NSG mice (n=8) was shorter than that in NOD/SCID mice (n=16) (72 d vs. 109.5 d, P=0.257, data not shown). Our data indicated that the successful establishment of HCC PDX was not associated with the experimental parameters. Therefore, we integrated the data of the two mouse strains for further analyses.

Clinicopathological parameters related to successful establishment of HCC PDX

We used key clinical parameters, including age, sex, presence of liver cirrhosis and hepatitis B surface antigen (HBsAg), tumor source (primary/recurrent), preoperative treatment, and preoperative serum AFP level, to explore their relationship to successful establishment. As shown in Table 3, a successful establishment was significantly related to age and preoperative serum AFP level. We observed that the engraftment rate was higher in younger patients (≤50 years) than in older patients (>50 years) (69.2% vs. 33.3%, P=0.016, Figure 4A). The engraftment rate was also higher

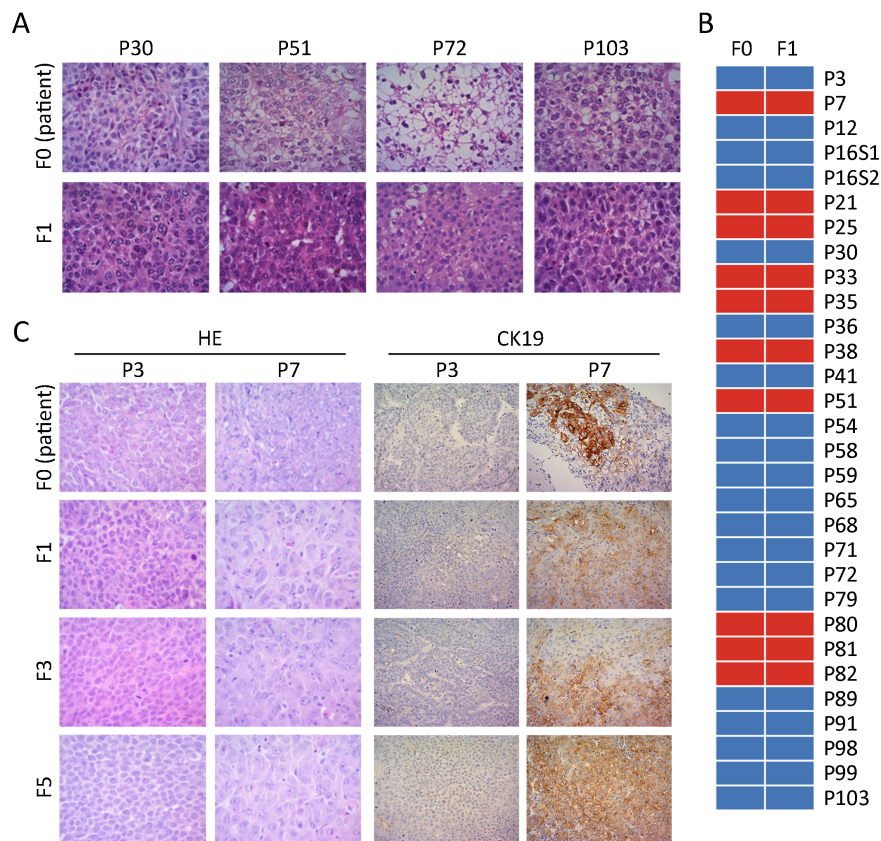


Figure 3 A comparison of histologic and molecular features between primary (F0) and PDX tumors. (A) Tumor section slides were stained using HE for comparing histology of four F1 PDX tumors with their corresponding F0 tumor; magnification 200 \times ; (B) Consistency of CK19 expression between F0 and F1 PDX tumors. Blue block, CK19-negative expression; red block, CK19-positive expression; (C) Two representative patient samples showing retained pathology and antibody (CK19) status as xenografts over several passages (F1–F3); magnification 200 \times . HE, hematoxylin and eosin; PDX, patient-derived xenograft; CK19, cytokeratin 19.

Table 2 Mouse strain related to establishment of HCC PDXs

Mouse strain	Successful	Failed	P
NOD/SCID	22	31	0.582
NSG	8	15	

HCC, hepatocellular carcinoma; PDX, patient derived xenograft; NOD/SCID, nonobese diabetic/severe combined immunodeficient mice; NSG, NOD/SCID/IL-2 γ -receptor null mice.

in the elevated AFP level (>20 ng/mL) subgroup than in the normal AFP level (\leq 20 ng/mL) subgroup (52.4% vs. 23.5%, $P=0.011$, *Figure 4A*). The PDX engraftment rate for poorly differentiated tumors was higher compared with that for well and moderately differentiated tumors (63.3% vs. 23.9%, $P=0.001$, *Figure 4B*, *Table 4*). Macro- (72.7%) and micro-vascular invasion (50.0%) also contributed to higher engraftment rates compared with non-vascular invasion (26.6%) ($P=0.011$, *Figure 4B*, *Table 4*). Histological subtyping was also associated with PDX

establishment ($P=0.043$). Therefore, the establishment of HCC PDX was closely related to tumor differentiation, vascular invasion, and histological subtyping.

Molecular parameters associated with successful establishment of HCC PDX

We primarily focused on the relationship between PDX establishment and molecular parameters. To identify the molecular features contributing to the establishment of PDX models, we evaluated HCC-related markers (AFP, GPC3), stemness-related markers (EpCAM, CD133 and CK19), and proliferation-related markers (Ki67). The results showed that positive expressions of CK19, CD133 and GPC3 were significantly associated with the successful establishment of HCC PDX models ($P=0.034$, 0.039 and 0.006, respectively, *Table 4*). For Ki67, the nucleus positive rates of samples were evaluated first. The median Ki67

Table 3 Clinical characteristics of patients related to establishment of HCC PDXs

Clinical characteristics	n (%)		P
	Successful (N=30)	Failed (N=46)	
Age (year)			0.016
≤50	9 (30.0)	4 (8.7)	
>50	21 (70.0)	42 (91.3)	
Sex			0.481
Male	26 (86.7)	37 (80.4)	
Female	4 (13.3)	9 (19.6)	
Liver cirrhosis			0.645
Yes	18 (60.0)	30 (65.2)	
No	12 (40.0)	16 (34.8)	
HBsAg			0.371
Yes	27 (90.0)	38 (82.6)	
No	3 (10.0)	8 (17.4)	
Primary tumor			0.745
Primary	26 (86.7)	41 (89.1)	
Recurrent	4 (13.3)	5 (10.9)	
Preoperative treatment			0.866
Yes	5 (16.7)	7 (15.2)	
No	25 (83.3)	39 (84.8)	
AFP (ng/mL)			0.011
≤20	8 (26.7)	26 (56.5)	
>20	22 (73.3)	20 (43.5)	

HCC, hepatocellular carcinoma; PDX, patient derived xenograft; HBsAg, hepatitis B surface antigen; AFP, alpha-fetoprotein.

nucleus positive rate was 39.5% (IQR: 30.0%–58.3%) in successful PDXs and 13.5% (IQR: 5.0%–37.3%) in failed PDXs. Furthermore, the cut-off value of Ki67 was set at 18.5% according to the Youden index, and the whole cohort was divided into Ki67-positive (>18.5%) and Ki67-negative (≤18.5%) subgroups. Finally, the data showed that positive expression of Ki67 was related to the successful establishment of HCC PDXs (P<0.001, Table 4). Therefore, the establishment of HCC PDX was closely related to the positive expression of CK19, CD133, GPC3 and Ki67.

GPC3/Ki67 phenotype promotes successful establishment of HCC PDX

To classify the various engraftment rates in PDXs, the significant parameters previously described, including age, preoperative serum AFP level, tumor differentiation, vascular invasion, histological subtyping, the expression of CK19, CD133, GPC3 and Ki67, were analyzed by multivariate logistic regression. The multivariate analysis showed that GPC3 and Ki67 were independent predictive factors for the successful establishment of HCC PDX (Table 5). Taking the two parameters together, we proposed a predictive phenotype for successful establishment of HCC PDX. As presented in Figure 5, tumors with GPC3/Ki67 phenotypes showed heterogeneous engraftment rates, with 71.9% in GPC3+/Ki67+ tumors, 30.8% in GPC3-/Ki67+ tumors, 15.0% in GPC3+/Ki67- tumors, and 0 in GPC3-/Ki67-

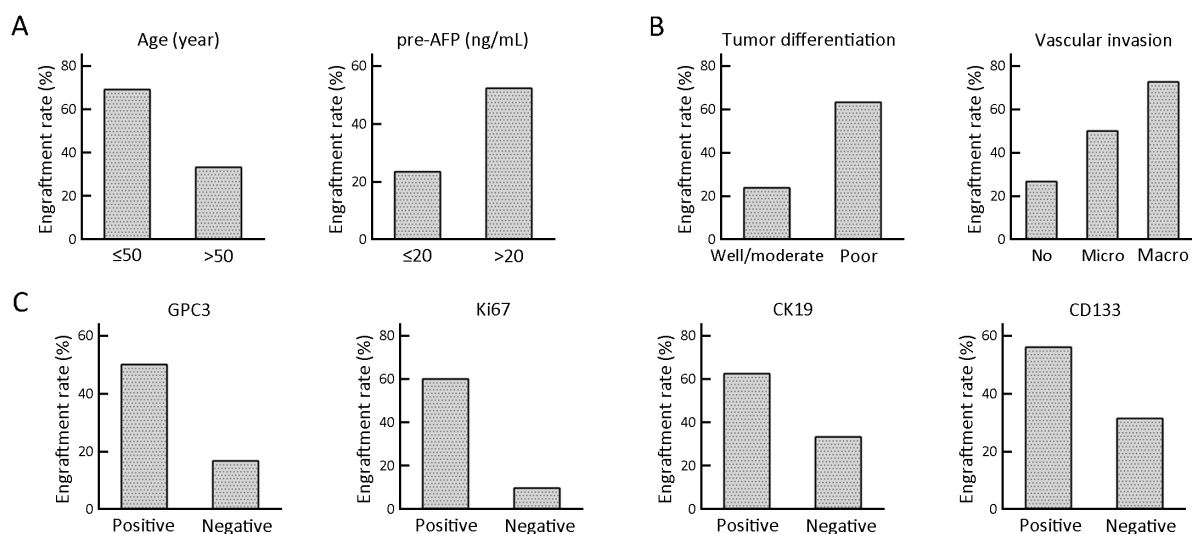


Figure 4 Clinical (A), pathological (B), and molecular (C) parameters associated with engraftment of HCC PDXs. HCC, hepatocellular carcinoma; PDX, patient-derived xenograft; pre-AFP, preoperative level of alpha-fetoprotein.

Table 4 Molecular-pathological parameters of tumors related to establishment of HCC PDXs

Parameters	n (%)		P
	Successful (N=30)	Failed (N=46)	
Tumor size (cm)			0.572
≤5	19 (63.3)	32 (69.6)	
>5	11 (36.7)	14 (30.4)	
Tumor differentiation			0.001
Well and Moderate	11 (36.7)	35 (76.1)	
Poor	19 (63.3)	11 (23.9)	
Satellite lesions			0.074
Yes	8 (26.7)	5 (10.9)	
No	22 (73.3)	41 (89.1)	
Vascular invasion			0.011
No	12 (40.0)	33 (71.7)	
Microvascular	10 (33.3)	10 (21.7)	
Macrovascular	8 (26.7)	3 (6.6)	
Histological subtyping			0.044
Microtrabecular	4 (13.3)	16 (34.8)	
Macrotrabecular	19 (63.3)	16 (34.8)	
Compact	2 (6.7)	8 (17.4)	
Pseudoglandular	5 (16.7)	6 (13.0)	
AFP expression			0.075
Positive	13 (43.3)	11 (23.9)	
Negative	17 (56.7)	35 (76.1)	
GPC3 expression			0.006
Positive	26 (86.7)	26 (56.5)	
Negative	4 (13.3)	20 (43.5)	
Ki67 expression			<0.001
Positive	27 (90.0)	18 (39.1)	
Negative	3 (10.0)	28 (60.9)	
CK19 expression			0.034
Positive	10 (33.3)	6 (13.0)	
Negative	20 (66.7)	40 (87.0)	
CD133 expression			0.039
Positive	14 (46.7)	11 (23.9)	
Negative	16 (53.3)	35 (76.1)	
EpCAM expression			0.555
Positive	11 (36.7)	20 (43.5)	
Negative	19 (63.3)	26 (56.5)	

The positive and negative expression of Ki67 was defined by the cut-off value of nucleus-positive rate. HCC, hepatocellular carcinoma; PDX, patient derived xenograft; AFP, alpha-fetoprotein; GPC3, glypican-3; CK19, cytokeratin 19; EpCAM, epithelial cell adhesion molecule.

tumors. In the 30 successfully established HCC PDXs, 76.7% (23/30) of PDXs exhibited the GPC3⁺/Ki67⁺

Table 5 Multivariate logistic regression of clinical and molecular pathological parameters for successful PDX establishment

Variables	HR	95% CI	P
GPC3	6.59	1.71–25.42	0.006
Ki67	16.76	4.12–68.07	<0.001

PDX, patient derived xenograft; GPC3, glypican-3; HR, hazard ratio; 95% CI, 95% confidence interval.

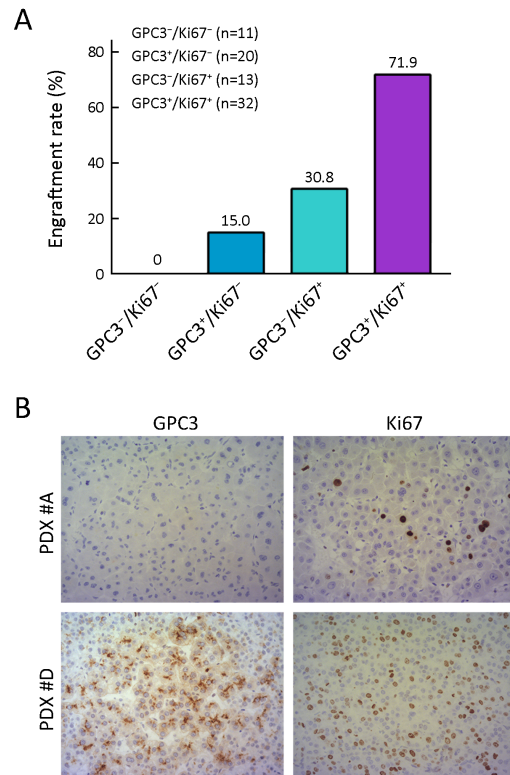


Figure 5 A comparison of engraftment rates between four phenotypes. (A) Group A, tumors with GPC3⁻ and Ki67⁻; Group B, tumors with GPC3⁺ and Ki67⁻; Group C, tumors with GPC3⁻ and Ki67⁺; Group D, tumors with GPC3⁺ and Ki67⁺. Subgroups of Ki67 were divided by the cut-off value of nucleus positive rate; (B) Representative phenotypes of PDX in groups A and D; magnification 200×. GPC3, glypican-3; PDX, patient-derived xenograft.

phenotype (Table 6). A combination of GPC3 and Ki67 had a predictive capability for successful PDX establishment, and the area under the curve was 0.828 (Figure 6). Therefore, the data indicated that PDXs can be classified based on GPC3/Ki67 phenotype, with the subtypes having heterogeneous engraftment rates, and GPC3⁺/Ki67⁺ phenotype could predict the successful establishment of HCC PDX.

Table 6 Four phenotypes of HCC patient derived xenograft models

Phenotypes	Successful [n (%)]	Failed [n (%)]
GPC3 ⁻ Ki67 ⁻	0 (0)	11 (23.9)
GPC3 ⁺ Ki67 ⁻	3 (10.0)	17 (36.9)
GPC3 ⁻ Ki67 ⁺	4 (13.3)	9 (19.6)
GPC3 ⁺ Ki67 ⁺	23 (76.7)	9 (19.6)

The subgroups of Ki67 were divided by the cut-off value of nucleus-positive rate.

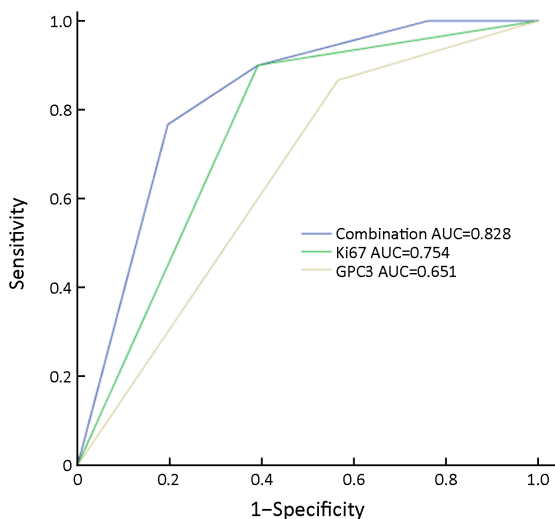


Figure 6 Receiver operating characteristic curve analysis of combination of Ki67 and GPC3 indicates strong predictive value for patient-derived xenograft establishment (AUC=0.828; 95% CI: 0.735–0.921). AUC, area under the curve; 95% CI, 95% confidence interval.

Discussion

PDXs are widely used for preclinical oncology research (10,12,21). The engraftment rate of PDXs varies among different cancer types. For example, the engraftment rate of HCC PDXs is lower than that of other cancer PDXs; colorectal and breast cancer as well as pancreatic ductal adenocarcinoma in particular have high engraftment rates (11,12). It is unclear whether there are any molecular pathological inconsistencies between successful and failed HCC PDXs; hence, in the present study, 76 HCC PDXs were used to explore pathological and molecular differences between these two.

In the cohort of HCC PDX models, the engraftment rate for successfully established PDXs was 39.47% (30/76). The engraftment rate was similar to that reported at another center (14). It has been shown that PDXs are

biologically and genetically similar to primary tumors (9,22). Consistent with these reports, the histological morphology and expression of key proteins in primary tumors were conserved in the HCC PDXs we established.

The successful establishment of PDX models is influenced by experimental, clinicopathological and molecular parameters. Choi *et al.* (23) investigated a few experimental parameters, including *ex vivo* times, tumor amount, mouse strain, and implantation site while making use of Matrigel. In the present study, all PDX tumors were subcutaneously implanted into the flanks of immunodeficient mice within 2 h, the only variable factor was the tumor-bearing mouse strain. Although NSG mice are reported to have a higher engraftment rate (12), in this study, there was no difference between NSG and NOD/SCID mouse strains in term of the engraftment rate. Therefore, the data of the two mouse strains were combined for subsequent analysis.

In the present study, the engraftment rate of HCC PDXs was significantly associated with age, preoperative AFP serum level, tumor differentiation, vascular invasion, and the histological subtyping (clinicopathological parameters). Hu *et al.* (14) reported that HCC PDX tumor engraftment was associated with poor tumor differentiation, lack of encapsulation, and large tumor size, which was partially consistent with our data. More importantly, we compared several critical molecular markers with the engraftment rate as well because HCC is highly heterogeneous at the molecular level (17), and different phenotypes and subtypes have disparate molecular expression patterns. Our data indicated that HCC PDX establishment was closely related to the expression of CK19, CD133, GPC3 and Ki67. Our data showed that a high positivity rate of Ki67 was remarkably associated with a high engraftment rate. Ki67 is widely recognized as a proliferative marker and is expressed in the cell nucleus during mitosis; however, it is not present during quiescence (15,24). Therefore, one possibility for the higher engraftment rate associated with Ki67 is that cells with a high proliferative ability have a greater chance to survive when tumor tissue samples are implanted into immunodeficient mice. Similar results were also shown in the PDX models of glioma and lung cancer (25,26). GPC3 is another striking marker for successful establishment of HCC PDXs. High expression of GPC3 has been associated with poor prognosis in patients with HCC (27). Recently, studies have demonstrated that GPC3 enhanced the proliferation of tumor cells by upregulating Wnt/ β -catenin, YAP and Hedgehog signaling (28,29).

We proposed a new classification based on the GPC3/Ki67 phenotype to predict successful establishment of HCC PDXs. The GPC3⁺/Ki67⁺ phenotype had the highest engraftment rate. Conversely, tumors with GPC3⁻/Ki67⁻ phenotypes were unlikely to establish PDXs. Therefore, GPC3⁺/Ki67⁺ phenotypes can predict successful PDX establishment. Additionally, among the established HCC PDXs, most of the PDXs exhibited a GPC3⁺/Ki67⁺ phenotype. When PDXs were used for large-scale *in vivo* screening, results of drug responses mainly come from tumors with GPC3⁺/Ki67⁺ phenotype. However, GPC3⁻/Ki67⁻ phenotype may be ignored, resulting in a selection bias that disrupts the results of drug efficacy. For example, some studies on PDXs will exclude data on these phenotypes and, therefore, are not able to accurately represent the HCC population. Oncologists should be aware of this bias when designing relevant studies. For tumors that cannot establish PDX models, patient-derived organoids (PDOs) may be suitable alternatives. Researchers have demonstrated the feasibility of efficiently generating biobanks of PDOs for all known molecular subtypes of breast, gastric and ovarian cancers (30-32). It seems that PDOs may have more potential applications in cancer research, drug development and personalized medicine than PDXs.

Conclusions

The successful establishment of HCC PDXs was significantly related to clinical and molecular pathological features. Tumors with the GPC3⁺/Ki67⁺ phenotype were most likely to successfully establish HCC PDXs.

Acknowledgements

This study was supported by grants from the National Science and Technology Major Project of China (No. 2017ZX10203205); the National Natural Science Funds for Distinguished Young Scholar of China (No. 81625003); Key Program National Natural Science Foundation of China (No. 81930016) and Key Research & Development Plan of Zhejiang Province (No. 2019C03050).

Footnote

Conflicts of Interest: The authors have no conflicts of interest to declare.

References

1. Forner A, Reig M, Bruix J. Hepatocellular carcinoma. *Lancet* 2018;391:1301-14.
2. Villanueva A. Hepatocellular carcinoma. *N Engl J Med* 2019;380:1450-62.
3. Allemani C, Weir HK, Carreira H, et al. Global surveillance of cancer survival 1995-2009: analysis of individual data for 25,676,887 patients from 279 population-based registries in 67 countries (CONCORD-2). *Lancet* 2015;385:977-1010.
4. Sun D, Cao M, Li H, et al. Cancer burden and trends in China: A review and comparison with Japan and South Korea. *Chin J Cancer Res* 2020;32:129-39.
5. Li Z, Zhu JY. Hepatocellular carcinoma: Current situation and challenge. *Hepatobiliary Pancreat Dis Int* 2019;18:303-4.
6. Llovet JM, Montal R, Sia D, et al. Molecular therapies and precision medicine for hepatocellular carcinoma. *Nat Rev Clin Oncol* 2018;15:599-616.
7. Nault JC, Galle PR, Marquardt JU. The role of molecular enrichment on future therapies in hepatocellular carcinoma. *J Hepatol* 2018;69:237-47.
8. Gould SE, Junttila MR, de Sauvage FJ. Translational value of mouse models in oncology drug development. *Nat Med* 2015;21:431-9.
9. Hidalgo M, Amant F, Biankin AV, et al. Patient-derived xenograft models: an emerging platform for translational cancer research. *Cancer Discov* 2014;4:998-1013.
10. Gao H, Korn JM, Ferretti S, et al. High-throughput screening using patient-derived tumor xenografts to predict clinical trial drug response. *Nat Med* 2015;21:1318-25.
11. Byrne AT, Alferez DG, Amant F, et al. Interrogating open issues in cancer medicine with patient-derived xenografts. *Nat Rev Cancer* 2017;17:632.
12. Jung J, Seol HS, Chang S. The generation and application of patient-derived xenograft model for cancer research. *Cancer Res Treat* 2018;50:1-10.
13. Gu Q, Zhang B, Sun H, et al. Genomic characterization of a large panel of patient-derived hepatocellular carcinoma xenograft tumor models for preclinical development. *Oncotarget* 2015;6:20160-76.
14. Hu B, Li H, Guo W, et al. Establishment of a

- hepatocellular carcinoma patient-derived xenograft platform and its application in biomarker identification. *Int J Cancer* 2020;146:1606-17.
15. Calderaro J, Ziol M, Paradis V, et al. Molecular and histological correlations in liver cancer. *J Hepatol* 2019;71:616-30.
 16. Goodman ZD. Neoplasms of the liver. *Mod Pathol* 2007;20(suppl 1):S49-60.
 17. Durnez A, Verslype C, Nevens F, et al. The clinicopathological and prognostic relevance of cytokeratin 7 and 19 expression in hepatocellular carcinoma. A possible progenitor cell origin. *Histopathology* 2006;49:138-51.
 18. Tang LH, Gonen M, Hedvat C, et al. Objective quantification of the Ki67 proliferative index in neuroendocrine tumors of the gastroenteropancreatic system: a comparison of digital image analysis with manual methods. *Am J Surg Pathol* 2012;36:1761-70.
 19. Andersen JB, Loi R, Perra A, et al. Progenitor-derived hepatocellular carcinoma model in the rat. *Hepatology* 2010;51:1401-9.
 20. Zhuo JY, Lu D, Tan WY, et al. CK19-positive hepatocellular carcinoma is a characteristic subtype. *J Cancer* 2020;11:5069-77.
 21. Lai Y, Wei X, Lin S, et al. Current status and perspectives of patient-derived xenograft models in cancer research. *J Hematol Oncol* 2017;10:106.
 22. Tentler JJ, Tan AC, Weekes CD, et al. Patient-derived tumour xenografts as models for oncology drug development. *Nat Rev Clin Oncol* 2012;9:338-50.
 23. Choi YY, Lee JE, Kim H, et al. Establishment and characterisation of patient-derived xenografts as preclinical models for gastric cancer. *Sci Rep* 2016;6:22172.
 24. Penault-Llorca F, Radosevic-Robin N. Ki67 assessment in breast cancer: an update. *Pathology* 2017;49:166-71.
 25. Zeng W, Tang Z, Li Y, et al. Patient-derived xenografts of different grade gliomas retain the heterogeneous histological and genetic features of human gliomas. *Cancer Cell Int* 2020;20:1.
 26. Lu D, Luo P, Zhang J, et al. Patient-derived tumor xenografts of lung squamous cell carcinoma alter long non-coding RNA profile but not responsiveness to cisplatin. *Oncol Lett* 2018;15:8589-603.
 27. Zhang J, Zhang M, Ma H, et al. Overexpression of glypican-3 is a predictor of poor prognosis in hepatocellular carcinoma: An updated meta-analysis. *Medicine (Baltimore)* 2018;97:e11130.
 28. Nishida T, Kataoka H. Glypican 3-targeted therapy in hepatocellular carcinoma. *Cancers (Basel)* 2019;11:1339.
 29. Kolluri A, Ho M. The role of glypican-3 in regulating Wnt, YAP, and Hedgehog in liver cancer. *Front Oncol* 2019;9:708.
 30. Sachs N, de Ligt J, Kopper O, et al. A living biobank of breast cancer organoids captures disease heterogeneity. *Cell* 2018;172:373-86.e10.
 31. Yan HHN, Siu HC, Law S, et al. A comprehensive human gastric cancer organoid biobank captures tumor subtype heterogeneity and enables therapeutic screening. *Cell Stem Cell* 2018;23:882-97.
 32. Kopper O, de Witte CJ, Lohmussaer K, et al. An organoid platform for ovarian cancer captures intra- and interpatient heterogeneity. *Nat Med* 2019;25:838-49.

Cite this article as: Zhuo J, Lu D, Wang J, Lian Z, Zhang J, Li H, Cen B, Wei X, Wei Q, Xie H, Xu X. Molecular phenotypes reveal heterogeneous engraftments of patient-derived hepatocellular carcinoma xenografts. *Chin J Cancer Res* 2021;33(4):470-479. doi: 10.21147/j.issn.1000-9604.2021.04.04